# ZERO-GRAVITY SLOSH ANALYSIS

*by T. W. Eastes, Y. M. Chang, C. W. Hirt, and J. M. Sicilian*

*presented at the 1985 Winter Annual Meeting, Miami, Florida, November 1985*

Rockwell International

Rocketdyne Division

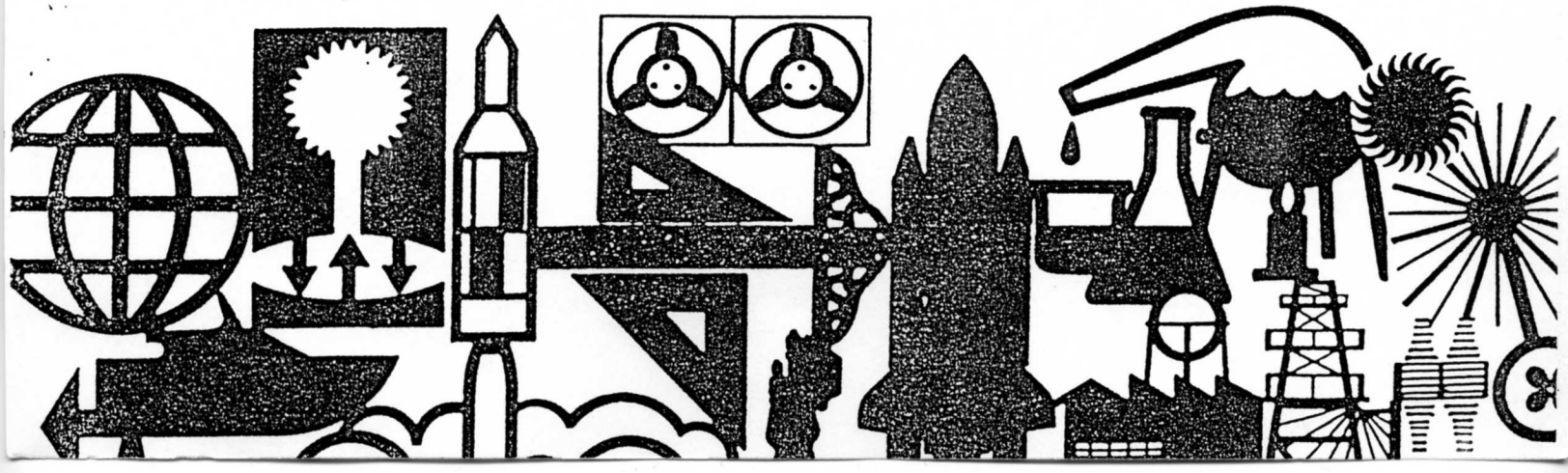

# ZERO-GRAVITY SLOSH ANALYSIS

*T. W. Eastes and Y. M. Chang*

*Rockwell International/Rocketdyne Division*
*Canoga Park, California*

*C. W. Hirt and J. M. Sicilian*

*Flow Science, Incorporated*
*Los Alamos, New Mexico*

ABSTRACT

Experimental results were used to anchor a newly developed three-dimensional, finite-difference hydrodynamics code that was designed to simulate large amplitude slosh in a container moving in a zero-g environment. The results of this anchoring are presented along with a brief description of the SOLA-SLOSH code (1), a description of the experiment, and a description of how the code was used to model pointing errors of a liquid-filled spacecraft during its space maneuvers.

INTRODUCTION

A major problem associated with spacecraft is control and management of liquid bulk. When liquids are stored in tanks with free ullages, pitch, yaw, or roll attitude maneuvers of the spacecraft result in combined rotational and translational acceleration of the tanks. After the maneuver, the liquids within the tanks can continue to move. This motion, called slosh, can cause erratic motion of the vehicle which often decays slowly, creating problems for the control system of the vehicle. Baffles and other slosh damping devices are frequently used to accelerate the decay rate of the residual motion. Yet, in some situations, accurate knowledge of the effect of slosh loads on the motion of the vehicle as a function of time is required for evaluation of control system adequacy. Furthermore, since the liquid may not be attached to the tank walls, knowledge of the center of gravity of the liquid bulk alone (as is often approximated by equivalent mechanical models) is of little use for vehicle control purposes.

For the present application, it was necessary to assess the pointing errors of the spacecraft due to slosh during Velocity Vector Correction (VVC) maneuvers, which are typically performed after a Single Axis Rotation (SAR) of the vehicle. Both SAR and VVC maneuvers cause motion of liquids within the propellant tanks, which in turn causes motion of the vehicle, requiring further VVC until pointing errors are under control.

Since the spacecraft operates in a zero-g environment, it was desirable to experimentally determine the impact of slosh-induced forces upon motion of the vehicle in that environment and assess the ability of the control system to correct errant motion. Existing drop towers are capable of only a few seconds of zero-g and can accommodate only small test articles. The zero-g environment of the Space Shuttle payload bay is desirable but is prohibitively expensive and requires a long lead time. NASA's KC-135A aircraft provides about 30 seconds of zero-g environment per session but is too small to contain the entire spacecraft. Therefore, it was necessary to model the distribution and motion of liquid within the tanks and predict loads on the tank walls. This model coupled with spacecraft rigid body dynamics and control system models could then calculate pointing errors of the vehicle.

Prediction of slosh forces and moments due to pitch, roll, and yaw maneuvers is quite difficult since generally these quantities are not only related to the initial free-surface configuration within the tank, the amount of liquid, the internal tank geometry, and the liquid properties, but also depend on the past history of the maneuver. The literature is filled with analytical solutions of free and forced slosh frequencies, velocity potentials, and force and moment amplitudes for various types of containers and excitations (see for example Ref. 2,3). These analyses, however, deal strictly with linearized Navier-Stokes equations and boundary conditions that apply only for low amplitude, sinusoidally excited slosh in a gravity field. They are limited to cases where past histories of excitations and boundary conditions are not important. Numerous mechanical (spring-mass-damper type) slosh models exist (see for example Ref. 3-6), including mass matrix models (7,8) and the pendulum model which is still widely used (see for example Ref. 9). However, these models are not applicable for tanks operating in a zero-g environment or having complex internal baffles, where the liquid bulk is expected to break up into a number of independently moving masses. A two-dimensional finite-difference code (10) exists that models the general free-surface motion associated

with large amplitude slosh. However, the complexity of the spacecraft tanks and maneuvers requires a three-dimensional description of the flow and acceleration fields. Therefore, Rockwell subcontracted to Flow Science Incorporated for SOLA-SLOSH (1), a three-dimensional, general-free-surface, viscous, finite-difference hydrodynamics code with limited compressibility.

To anchor the new code for its desired application, a series of experiments was proposed to simulate tank-slosh dynamics in a zero-g environment aboard NASA's KC-135A aircraft. The experiments chosen required the 90-degree, single-axis rotation of a partially filled propellant tank. The experiments were performed in two phases: Phase I (11) in August 1983 and Phase II (12) in November 1983.

Based on SOLA-SLOSH, Rockwell constructed computer models of the Phase I and II tanks with different baffle configurations and fill levels. Measured acceleration time histories from several tests were digitized and applied to the models. The model-generated force- and moment-time histories were then compared to their experimentally measured counterparts. Agreements were very good and served to anchor the models as well as the code. Agreements between the code and linear slosh theory for low amplitude slosh in a gravity field (13,14) were excellent and are published elsewhere (15,16).

After verification of SOLA-SLOSH and the tank models with experimental results, Rockwell integrated the tank models with the spacecraft rigid body dynamics/control system model. The dynamics/control system model provides the slosh model with the tank accelerations. The slosh model, in turn, feeds back slosh forces and moments, which (in addition to the rocket engine firings) determine the dynamics of the spacecraft and thus the tank accelerations. The control system then calculates the pointing error and determines the appropriate velocity vector correction maneuver.

## SOLA-SLOSH CODE

The forces generated by propellant motion are affected by many things, including the spin and acceleration of the vehicle, the location of the propellant, the geometry of the tank, the properties of the propellant, and the reaction of the vehicle to these forces. SOLA-SLOSH has been developed to permit simulation of these features for most situations of interest in spacecraft. The code SOLA-SLOSH has evolved from the well-known Marker-and-Cell (MAC) finite difference technique (17,18), which uses pressure and velocity as primary dependent variables. SOLA-SLOSH is a three-dimensional extension of the two-dimensional solution algorithm, SOLA-VOF (10), which simulates the general free-surface motion of a liquid. SOLA-SLOSH has several additional features which accommodate liquid slosh simulation including: (1) a generalized obstacle, porous baffle, and curved wall simulation capability which uses a fractional area/volume method, (2) a generalized routine for input of motion forcing functions simulating generalized noninertial tank accelerations, and (3) a routine for calculation of forces and moments created by the liquid motion. In this section we describe the aforementioned features and their associated numerical techniques that support propellant motion simulations. Greater detail governing each aspect of the resultant computer code is available elsewhere (1).

SOLA-SLOSH solves, by finite-difference techniques, the three-dimensional Navier-Stokes equations for the flow of an incompressible (or slightly compressible) fluid with multiple free surfaces. Calculations are performed and results are presented, in an accelerating reference frame, fixed with respect to the propellant tank. The solution algorithm is similar to that implemented in SOLA-VOF (10) which uses a staggered mesh with implicit pressure gradient to efficiently solve low-speed flow problems. The Volume of Fluid (VOF) technique (19) is used to track free-surface motions.

Forces and moments are evaluated by summing the pressure-area product for each cell in the computational mesh. Therefore, the effects of forces not represented by the pressure are ignored in this evaluation. In particular, viscous shear stresses, which are paramount for long-term energy dissipation in spinning systems, are omitted.

Several features of SOLA-SLOSH assist in the accurate representation of tank geometry. Either Cartesian or cylindrical coordinates may be employed. However, Cartesian coordinates are generally preferred for calculations involving nonaxisymmetric flows because of numerical difficulties associated with a cylindrical axis. A variable-size grid is available that permits resolution of important local detail while minimizing the computational cost. Finally, partial area and volume fractions represent the tank geometry on a scale finer than the computational mesh itself, as described below.

The SOLA-SLOSH difference equations acknowledge the possibility that portions of mesh-cell faces and volumes may be obstructed from flow by geometric features of the tank. Easily used generators permit the user to specify the geometry of the tank walls and interior baffle locations. These generators calculate the blocked area and volume fractions for every mesh cell. For example, if the tank is spherical with an inside diameter of 100 cm., the user simply specifies the function

$$F_1 = x^2 + y^2 + z^2 - 10^4$$

The equation, $F_1 = 0$, describes the boundary. If additionally, there is a diametrical baffle with an area fraction of 0.5, the user defines its porosity (0.5) and its location via

$$F_2 = z$$

The closest cell faces to the solution of $F_2 = 0$ describe the baffle. SOLA-SLOSH then calculates the area and volume fractions associated with each cell in the computational mesh.

Because the computational mesh is not an inertial reference frame, an acceleration field is experienced by the fluid. This acceleration is given by the negative of

$$\overrightarrow{ACC} = \dot{\vec{U}} + \dot{\vec{\Omega}} \times (\vec{r}-\vec{R}) + 2\vec{\Omega} \times \vec{u} + \vec{\Omega} \times (\vec{\Omega} \times (\vec{r}-\vec{R})) \qquad (1)$$

The evaluation of $\overrightarrow{ACC}$ is broken into two parts in SOLA-SLOSH. The first is the representation of the reference-frame motion and the second the evaluation of required local values of the acceleration for each velocity component at each cell of the mesh.

The motion of the reference frame is expressed in terms of the parameters:

$\vec{R}$ = location of a stationary reference point in the coordinates of the tank-fixed reference frame

$\dot{\vec{U}}$ = absolute linear acceleration of the reference frame

$\vec{\Omega}$ = absolute angular velocity of the reference frame expressed about the point R

$\dot{\vec{\Omega}}$ = absolute angular acceleration of the reference frame about the point R

These vectors are evaluated in terms of the noninertial coordinates in which the mesh is specified. In general, they vary with time (except for the fixed point $\vec{R}$). The computer code must be given these accelerations by the user for each new problem. Evaluation of the local accelerative force is then performed in three subroutines, one evaluating each vector component. Using Equation (1) and the local velocity $\vec{u}$ and position $\vec{r}$, these routines evaluate local acceleration components in a general way and do not require modification.

Free surfaces are represented in SOLA-SLOSH by the VOF algorithm (19). VOF assigns a fluid fraction to each mesh cell. These are initialized by a generator similar to that used for the tank geometry. The fluid fraction evolves through the numerical solution of a transport equation using special differencing schemes developed to minimize numerical diffusion effects. A specified-pressure boundary condition is imposed at the free surface together with zero tangential stress conditions. Imposition of these boundary conditions requires knowledge of the surface orientation. Evaluation of surface-tension forces additionally requires calculation of the surface curvature. Orientation and curvature are evaluated by examination of the fluid fractions in the 26 cells surrounding each cell that contains a free surface.

One problem, difficult to address in general, is the initial configuration of free surface in the system. A limited surface-initialization procedure is included in SOLA-SLOSH. This procedure evaluates the equilibrium surface location under specified, constant accelerations. The procedure is limited to surfaces that are nearly perpendicular to the z axis (those that can be expressed in the form $z = S(x,y)$). Therefore, problems that are initialized from zero-g conditions must be described through input. This can be obtained from experimental data or by a worse case analysis for bounding calculations.

The difference equations for the evaluation of viscous shear-stress terms account for the presence of blocked volumes and areas, and are written to easily include the effects of varying viscosity, although no models for nonuniform viscosity (such as a turbulence model) are presently included in SOLA-SLOSH.

SOLA-SLOSH results have been compared with simple experiments and linear analysis for a range of problems (15,16). Of particular interest are comparisons with linear free-surface theory for sloshing in spherical and cylindrical tanks in a gravitational field (13,14). These comparisons show nearly exact agreement if corrected for the effects of nonlinear terms. Excellent results have been obtained using quite coarse (10 x 10 x 10) mesh structures. Other comparisons establish the code's correctness for modeling particular phenomena. For example, the simulation of Poiseuille flow displays its accuracy for viscous shear and pressure gradient effects when shear layers are adequately resolved.

## EXPERIMENTS

The experiments performed were 90-degree, (SARs) of a partially filled propellant tank (Fig. 1). A full-scale Plexiglas tank partially filled with a blue dyed liquid was used so that the liquid motion could be recorded on movie film and to aid in determining the initial free-surface configuration. The experiments were performed on NASA's KC-135A aircraft which flies parabolas to provide the required zero-g (within 0.05 g) environment for about 30 seconds in each parabola. The tanks were instrumented in all six degrees of freedom with accelerometers, gyrometers, and load cells to detect motion and forces. These data were

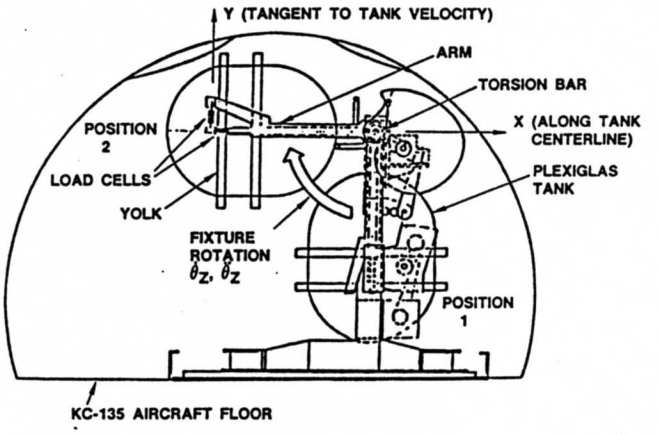


Fig. 1. Rotational Test Apparatus in KC-135 Aircraft

recorded onto magnetic tape for processing at a later time. Selected data were recorded on strip chart recorders for on-the-spot examination of key parameters to determine the validity of a given test. In postprocessing of the data, effects of dry tank inertia were subtracted from the data so that the resulting time histories of forces and moments were due solely to the liquid.

The experiments were conducted in two phases. Phase I testing (11), performed in August 1983, used a large tank (Fig. 2) with various fill levels, baffle configurations, and angular accelerations and used water as the liquid. Phase II testing (12), performed in November 1983, used a smaller tank (Fig. 3) with various fill levels, and angular accelerations and used Freon TF as the liquid. The tank used in Phase II testing has a shorter cylindrical section than the tank used in Phase I testing. In Phase II, the baffle configuration was fixed following a preliminary evaluation of baffle performance in Phase I testing. In Phase I testing a solid Plexiglas structure replaced the surface tension screens and the Propellant Acquisition Device (PAD) region contained no liquid. However, in Phase II testing, the PAD contained liquid with an actual surface tension screen serving to

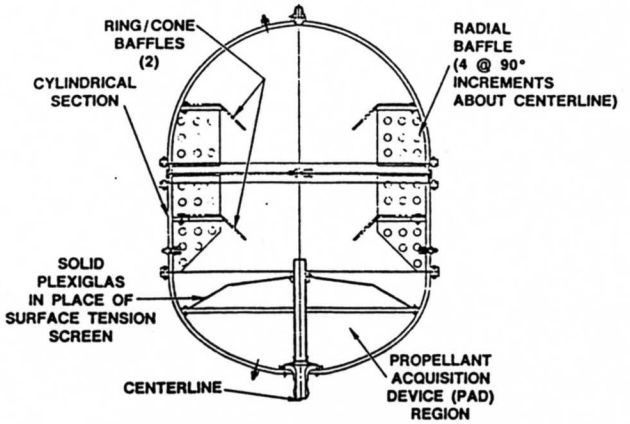


Fig. 2. Phase I Tank Cross Section

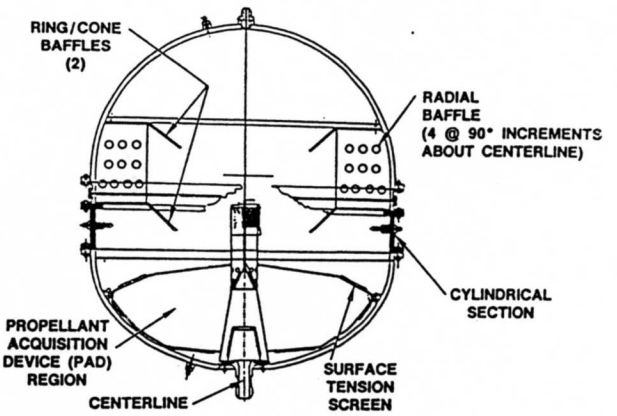


Fig. 3. Phase II Tank Cross Section

retain liquid in that region. The test apparatus for the SAR maneuvers was the same in both phases with some instrumentation and procedural improvements in Phase II.

In the SAR experiments (Fig. 1), the tank was to be rotated from its initial down position (Position 1) at constant angular acceleration through the first 45 degrees and decelerated at constant angular acceleration of same magnitude through another 45 degrees until it stopped at its final up position (Position 2). Typical angular-velocity and angular-acceleration time histories are shown in Fig. 4a and 4b, respectively. Angular-acceleration values used for testing were 0.0, 18.1, 23.2, and 28.3 deg/sec$^2$.

Although the yolk device attached to the tank was designed to be rigid, the torsion bar and the supporting arms (Fig. 1) driving the yolk/tank assembly were not and were later found to have a structural resonance at approximately 3 Hz. Since measured acceleration time histories were applied directly to the computational model for the simulated test cases, this did not impair the code anchoring procedure.

According to test plans, the liquid was initially supposed to be in the bottom of the tank due to the heavier gravity field (about 2 g) created just prior to the parabolic maneuver of the aircraft. However, this was not always the case as the aircraft occasionally overshot its zero-g goal inducing a slightly reversed gravity field. This caused some liquid to move toward the top of the tank. This is difficult to model as is discussed in later sections.

## TANK MODELS

The computational tank models were constructed to simulate the internal geometries of the physical tanks including the baffles. The most important characteristics of the problem were assumed to be mass distribution and motion of the propellant within the tank. Furthermore, the required outputs from the simulation are integrated quantities, being forces and moments. Therefore, a relatively coarse grid was used. The justification for use of the coarse grid is discussed in the next section. The finite difference grids used to model the tanks for Phase I and Phase II are shown in Fig. 5 and 6, respectively. As seen from comparison to the actual tanks in Fig. 2 and 3, the geometries are suitably modeled with a minimum number of grid cells. The grid line spacing used in the tank models was specified to maintain relative uniformity of grid cells and coincide with geometric features of the tanks.

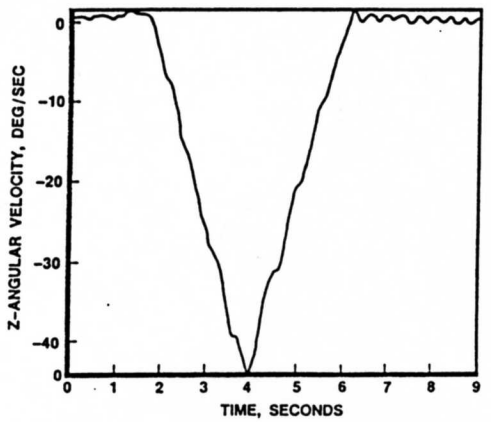


ANGULAR VELOCITY

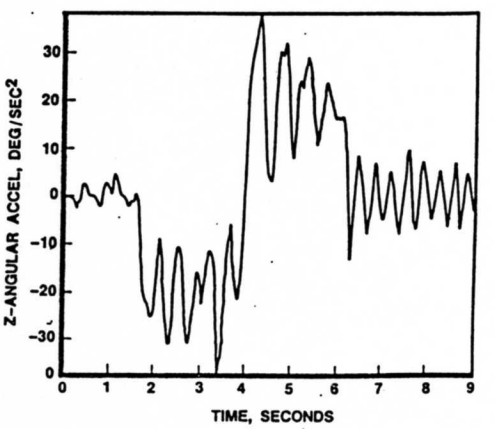


ANGULAR ACCELERATION

Fig. 4. Typical Time History for KC-135 Experiment

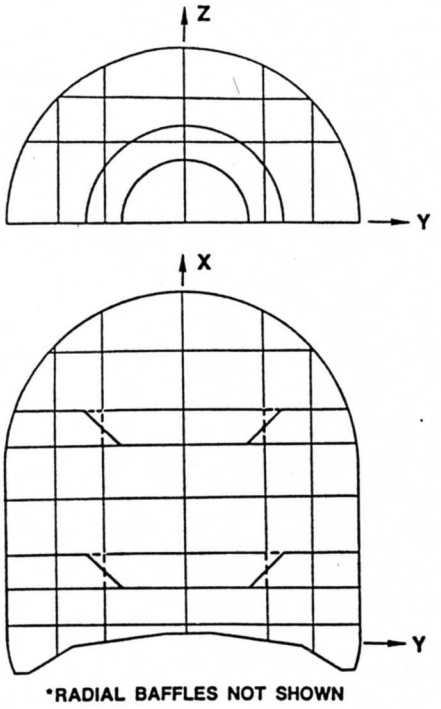


Fig. 5. Phase I Tank Model Grid*

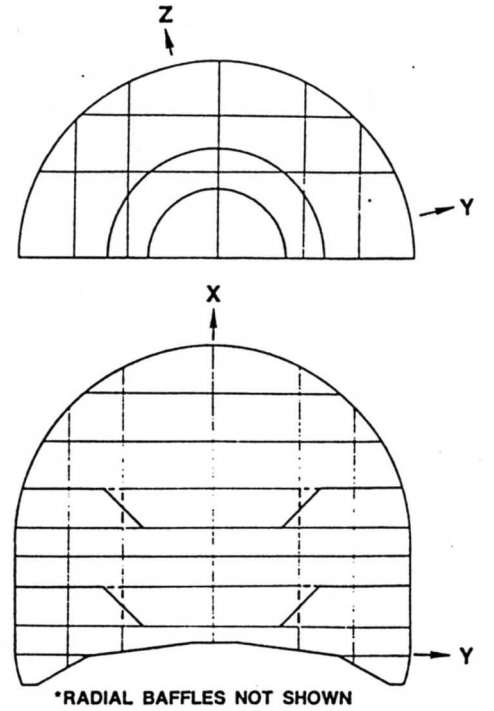


Fig. 6. Phase II Tank Model Grid*

Due to symmetry of the tank with respect to the SAR maneuver for Phase I experiments, the corresponding tank model was halved thus cutting computational costs in half. However, in Phase II experiments, the lateral baffles did not coincide with the plane of symmetry (offset 11.25 degrees) and the entire tank was modeled to accommodate the nonsymmetric flow field.

Another simplification to the model was exclusion of the propellant acquisition device region from the computational domain. This is because the PAD was empty in Phase I. In Phase II, forces and moments due to motion of the stagnant liquid (relative to the tank) in that region are more easily, yet accurately, modeled as if they were due to motion of a "frozen mass." Also in the Phase II tank, a small diameter cylindrical structure associated with the PAD was omitted from the model, since its effect on the flow field was negligible compared to other internal structures of the tank, such as baffles.

All boundaries, baffles, and the initial free-surface configuration are defined by generators (see code description section). The curved portions of the tank are treated using the fractional area/volume method thus eliminating erroneous effects created by stairstep-type boundaries as in SOLA-VOF (10). The density, viscosity, and speed of sound of the liquid are model inputs as well and were appropriately input to correspond to the test liquid properties for each phase of testing. As indicated in the experiment description section, the initial free-surface position was difficult to assess, but for modeling purposes was assumed to be normal to the x-axis with the liquid in the bottom of the tank. The justification for this assumption is discussed in the next section.

The baffles (shown as solid lines inside the closed boundary in Fig. 5 and 6) are also modeled using the fractional area method, but must conform to the nearest available grid surfaces (shown as dotted lines when not coincident with physical baffles in Fig. 5 and 6). Due to the 11.25-degree offset of the radial baffles in Phase II experiments, a simple coordinate system rotation was performed on accelerations before they were applied to the model so that the baffles were coincident with grid surfaces.

Eight Phase I tests and four Phase II tests were selected for simulation. Experimentally measured tank motion data (i.e. linear accelerations, angular accelerations, and angular velocities) were digitized and applied to the tank models. The resultant forces and moments due to the computational models were then compared to their experimentally measured counterparts (Fig. 7).

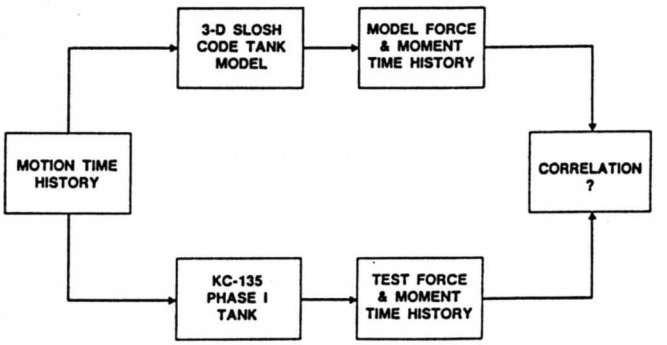


Fig. 7. Code Anchoring with KC-135 Testing

## DISCUSSION AND RESULTS OF EXPERIMENTAL ANCHORING

Comparisons of the experimental force and moment time histories with the model's prediction of these quantities are shown for two selected cases in Fig. 8 9, and 10. In general, model/experiment correlations are excellent for both Phase I and Phase II with few exceptions.

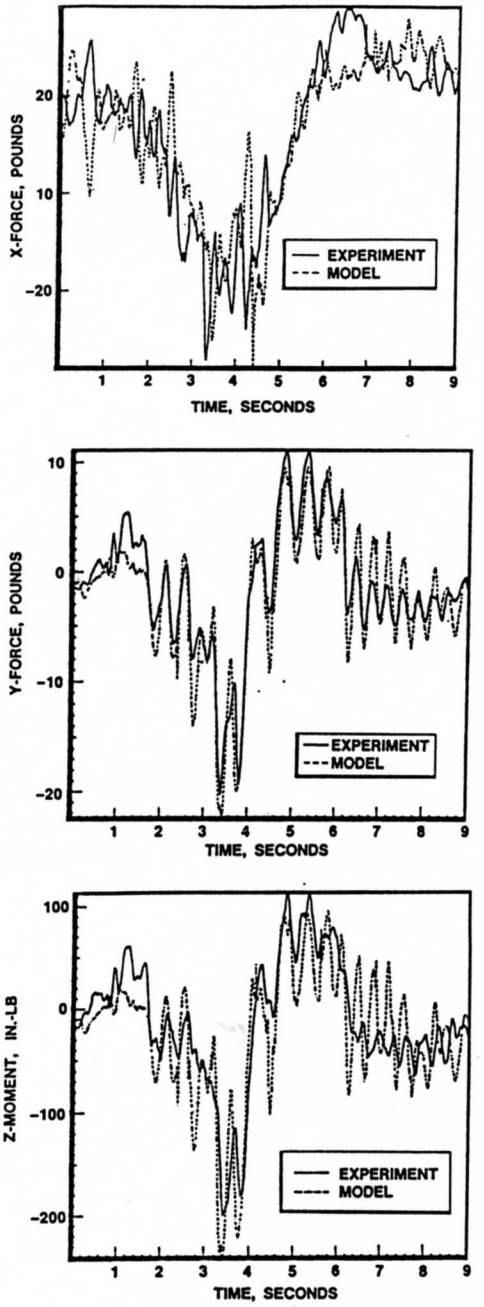


Fig. 8. Model/Experiment Comparison (Phase I, Series A3-1, Run 3, 60 Percent Fill, No Baffles)

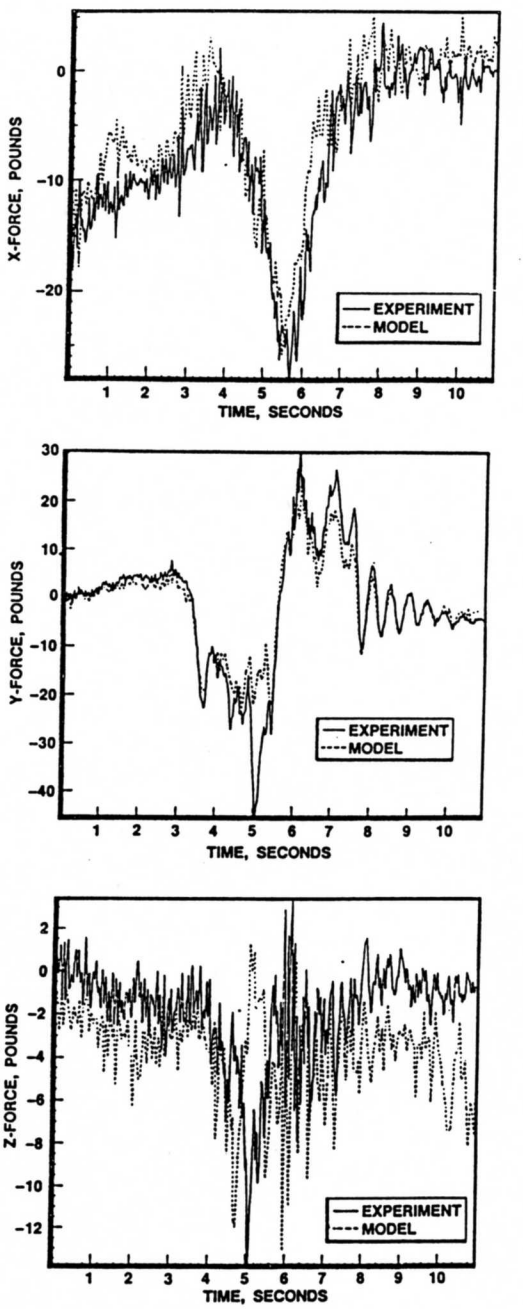


Fig. 9. Model/Experiment Comparison (Phase II, Series C2, Run 4, 40 Percent Fill, Ring/Cone Baffles)

The dynamic movement of a gas-liquid system, such as a propellant tank, is typically influenced by a combination of capillary forces, body forces, viscous forces, and inertia forces. Since slosh forces and moments are integrated quantities, many aspects of fluid flow normally considered important to other engineering applications were neglected. Liquid velocity and acceleration within the propellant tanks fluctuated wildly, so dimensionless parameters are calculated using estimations of their RMS values. The Reynolds number is high enough (in the order of $10^5$ based on tank radius) so that viscous drag may be neglected. The Weber number (defined as the ratio of inertial forces to capillary forces), based on the tank radius, is in the order of $10^3$, rendering capillary forces negligible compared to inertial forces. The Bond number (defined as the ratio of body forces to capillary forces), based on the tank radius, is in the order of $10^3$, and thus, capillary forces are negligible compared to body forces also. Therefore, the primary motion of liquid within our propellant tanks is due to fluctuating inertial and body forces, giving rise to a simple mass distribution and motion problem. Since both viscous and surface tension effects are negligible, use of fine grids to resolve them is not necessary. Sicilian and Hirt (15) have shown that agreement is slightly improved for simulation of one test case using a fine-grid model, but does not warrant the additional cost.

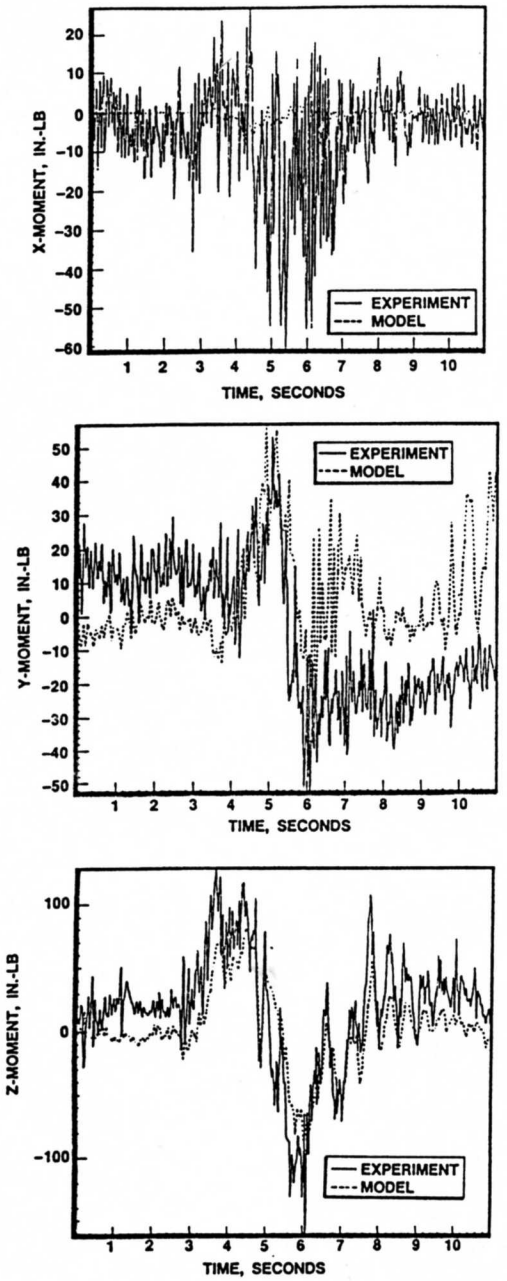


Fig. 10. Model/Experiment Comparison (Phase II, Series C2, Run 4, 40 Percent Fill, Ring/Cone Baffles)

A problem associated with the simulation was initialization of the free-surface position. As previously stated, an attempt was made in the experiments to position the liquid with its free-surface normal to the x-axis with the liquid in the bottom of the tank. Review of movies taken during the experiment indicate that the initial free-surface configuration was not so ideal and difficult to define. Subsequently, simulations were performed assuming the initial free-surface normal to the x-axis. Yet, agreements between the model and the experiment did not appear to be significantly affected. This is probably because the liquid was only slightly perturbed from the ideal situation. Therefore, when the integrated quantities of force and moment were calculated, local perturbations were averaged out in the integration process.

In Phase II testing, the PAD region (see Fig. 3) contained liquid, so the model was modified to include effects of this liquid moving as a frozen mass instead of flowing through the surface tension screen between the PAD region and the rest of the tank. However, the code can accommodate flow through porous screens as discussed in the code description section. The modeling results confirm that no substantial flow occurs through the surface tension screen.

A numerical problem encountered was associated with the coarseness of the finite-difference mesh. When a cell becomes completely filled with liquid, the code immediately imposes a zero divergence condition, which was not required in the previous time step. This may require rapid changes in the liquid inflow from neighboring cells. Because the momentum associated with the liquid inflow is larger in a coarse mesh, the pressure required to change the momentum is also larger. These increases in pressure are reflected in the model's predicted force and moment traces as spikes. The spikes do not appear to affect the solution following their occurrence. Due to their shortness of duration and relatively large magnitude, the force and moment spikes are easily discernable and removed. The insertion of compressibility in the solution is quite beneficial in depressing their magnitude and has been applied to all simulations.

No other attempt was made to correct the simulations for the aforementioned experimental errors and modeling assumptions. Nonetheless, agreement between the simulations and experimental data is excellent.

## INTEGRATION OF SLOSH MODEL WITH DYNAMICS/CONTROL SYSTEM MODEL

To evaluate pointing errors of the spacecraft, slosh models representing the propellant tanks were combined with the vehicle dynamics/control system model into a single "closed-loop" model. The vehicle dynamics/control system model contains rigid body dynamics equations for the spacecraft as well as provisions for simulating reactions from various attitude control engine firings. At each time step of the simulation, the dynamics/control system model passes accelerations (linear acceleration, angular acceleration, and angular velocity) experienced at the spacecraft's nominal center of mass to the slosh model, which then calculates the slosh forces and moments experienced by each tank model and passes these back to the dynamics/control system model. In the dynamics/control system model the slosh forces and moments are added to those due to rocket engine firings to determine the accelerations of the spacecraft's nominal center of mass for the next time step. This completes the closed-loop coupling of the models in each time step. By marching the time step in this manner, the spacecraft pointing error can then be calculated during and after various vehicle SAR and VVC maneuvers of a typical duty cycle.

This combined model was given to another Rockwell division for purposes of evaluating the pointing errors of a spacecraft. There has been no reported difficulty with the numerical spikes (discussed in the previous section) in their applications of this combined model. Results of that investigation are presented in Ref. 20

## CONCLUSIONS

SOLA-SLOSH has demonstrated its accuracy for simulating the effects of large amplitude, zero-g slosh and represents a major step in making slosh analysis a deterministic, well-defined science. Another vital insight gained was that in spite of an extremely coarse mesh, excellent agreement between the experiment and code prediction of integrated quantities (i.e., forces and moments) was obtained. This indicates that the flow problem was influenced by fluctuating inertia and body forces rather than viscous and capillary forces. Perturbations of the initial free surface about an assumed equilibrium position were also determined to be of little importance in calculation of integrated quantities.

## ACKNOWLEDGMENTS

This work was sponsored by the United States Air Force under contract number F04704-83-C-0004. The authors wish to thank Paul Reiser, Jim Fenwick, Phil Shigemura and other Rocketdyne colleagues for their support to the program. Thanks also go to Bob Laurensen, Leo Valla, and other McDonnel Douglas Astronautics Company and National Aeronautics and Space Administration colleagues for their excellent work on the zero-g experiments. We also wish to thank Art Katz, Rick Boyer, and Tony Mucci of the Autonetics Division of Rockwell International for their support on the integration effort of the vehicle dynamics/control system model and the slosh model, and Terry Miwa of TRW for his helpful suggestions.

## REFERENCES

1. Hirt, C. W., Sicilian, J. M., and Harper, R. P., "SOLA-SLOSH: A Solution Algorithm for Transient Three-Dimensional Flows," Flow Science, Inc. Report FSI-83-00-3, 1983.

2. Satterlee, H. M. and Reynolds, W. C., "The Dynamics of the Free Surface in Cylindrical Containers Under Strong Capillary and Weak Gravity Conditions," Technical Report LG-2, Thermosciences Division, Dept. of Mechanical Engineering, Stanford University, Stanford, California, 1963.

3. Abramson, H. N., ed., "The Dynamic Behavior of Liquids in Moving Containers," NASA Office of Scientific and Technical Information SP-106, Washington, 1966.

4. Chu, W. H., "Low-Gravity Fuel Sloshing in an Arbitrary Axisymmetric Rigid Tank," J. Applied Mechanics, Vol. 37, No. 3, Transactions of the ASME, Series E, Vol. 92, 1970, p. 828.

5. Bauer, H. F. "Nonlinear Mechanical Model for Description of Propellant Sloshing," AIAA J., Vol. 4, No. 9, 1966, p. 1662.

6. Yeh, G. C. K., "Free and Forced Oscillations of a Liquid in an Axisymmetric Tank at Low-Gravity Environments," J. Applied Mechanics, Vol. 34, No. 1, Transactions of the ASME, Vol. 89, Series E, 1967, p. 23.

7. Hunt, D. A., "Discrete Element Structural Theory of Fluids," AIAA J., Vol. 9, No. 3, 1971, p. 457.

8. Berry, R. L., Demchak, L. J., Tegart, J. R., and Craig, M. K., "An Analytical Tool for Simulating Large Amplitude Propellant Slosh," AIAA Paper 81-0500-CP, presented at 22nd Structures, Structural Dynamic & Materials Conference, Atlanta, Georgia, April 1981.

9. Sayar, B. A., and Baumgarten, J. R., "Linear and Nonlinear Analysis of Fluid Slosh Dampers," AIAA J., Vol. 20, No. 11, 1982, p. 1534.

10. Nichols, B. D., Hirt, C. W., and Hotchkiss, R. S., "SOLA-VOF: A Solution Algorithm for Transient Fluid Flows with Multiple Free Boundaries," Los Alamos Scientific Laboratory Report LA-8355, 1980.

11. Valla, L. B. "Propellant Storage Assembly Test 110/Phase I Low-G Propellant Residual Motion Test Report," McDonnell Douglas Astronautics Company, St. Louis Division Report TN-E237-37, 1984.

12. Valla, L. B. "Propellant Storage Assembly Test 110/Phase II Low-G Propellant Residual Motion Preliminary Data Submittal," McDonnell Douglas Astronautics Company, St. Louis Division Report TN-E237-46, 1984.

13. Hunt, B., and Priestly, N., "Seismic Water Waves in a Storage Tank," Bulletin of Seismological Society of America, Vol. 68, No. 2, 1978, p. 487.

14. Budiansky, B., "Sloshing of Liquids in Circular Canals and Spherical Tanks," J. of the Aero/Space Sciences, Vol. 9, No. 3, 1960, p. 161.

15. Sicilian, J. M. and Hirt, C. W., "Development and Testing of the SOLA-SLOSH Computer Program," Flow Science, Inc. report FSI-84-18-2, 1984.

16. Sicilian, J.M. and Hirt, C. W., "Numerical Simulation of Propellant Sloshing for Spacecraft," ASME Winter Annual Meeting, Forum on Unsteady Flow, G00259, 1984, p. 10.

17. Harlow, F. H. and Welch, J. E., "Numerical Calculations of Time-Dependent Viscous Incompressible Flow of Fluid with Free Surface," Physics of Fluids, Vol. 8, No. 12, 1965, p. 2182.

18. Welch, J. E., Harlow, F. H., Shannon, J. P., and Daly, B. J., "The MAC Method: A Computing Technique for Solving Viscous, Incompressible, Transient Fluid-Flow Problems Involving Free Surfaces," Los Alamos Scientific Laboratory Report LA-3425, 1966.

19. Nichols, B. D. and Hirt, C. W., "Volume of Fluid (VOF) Method for the Dynamics of Free Boundaries," J. Computational Physics, Vol. 39, No. 3, 1981, p. 201.

20. Mucci, T., "Analysis of Spacecraft Pointing Vector Errors," Autonetics Strategic Systems Division Report to be released, 1985.